J|A|C|S
ARTICLES
Published on Web 12/31/2005

Infrared Spectroscopy of Hydrated Amino Acids in the Gas Phase: Protonated and Lithiated Valine

Anthi Kamariotis,[†] Oleg V. Boyarkin,[†] Sébastien R. Mercier,[†] Rainer D. Beck,[†] Matthew F. Bush,[‡] Evan R. Williams,[‡] and Thomas R. Rizzo*,[†]

Contribution from the Laboratoire de Chimie Physique Moléculaire, Ecole Polytechique Fédérale de Lausanne, CH-1015 Lausanne and the Department of Chemistry, University of California, Berkeley, California 94720-1460

Received September 3, 2005; E-mail: thomas.rizzo@epfl.ch

Abstract: We report here infrared spectra of protonated and lithiated valine with varying degrees of hydration in the gas phase and interpret them with the help of DFT calculations at the B3LYP/6-31++G** level. In both the protonated and lithiated species our results clearly indicate that the solvation process is driven first by solvation of the charge site and subsequently by formation of a second solvation shell. The infrared spectra of Val·$Li^+(H_2O)_4$ and Val·$H^+(H_2O)_4$ are strikingly similar in the region of the spectrum corresponding to hydrogen-bonded stretches of donor water molecules, suggesting that in both cases similar extended water structures are formed once the charge site is solvated. In the case of the lithiated species, our spectra are consistent with a conformation change of the amino acid backbone from syn to anti accompanied by a change in the lithium binding from a NO coordination to OO coordination configuration upon addition of the third water molecule. This change in the mode of metal ion binding was also observed previously by Williams and Lemoff [*J. Am. Soc. Mass Spectrom.* **2004**, *15*, 1014−1024] using blackbody infrared radiative dissociation (BIRD). In contrast to the zwitterion formation inferred from results of the BIRD experiments upon addition of a third water molecule, our spectra, which are a more direct probe of structure, show no evidence for zwitterion formation with the addition of up to four water molecules.

I. Introduction

Water plays a central role in determining protein structure through its ability to moderate electrostatic forces. At physiological pH, most biological molecules contain charged groups and the competition between charge solvation by water and by the molecule itself helps determine the subtle energetic balance that leads to the stabilization of a particular conformation.[1−6] Understanding the detailed role of these forces can be facilitated by removing biological molecules from their condensed phase environment[7] and systematically studying them in the gas phase with varying degrees of hydration.[1−6,8−18]

A clear example where solvent plays a crucial role is in zwitterion formation. In aqueous solution at physiological pH, most amino acids are in their zwitterionic form, where the carboxylic acid at the C-terminus is deprotonated and the amino group at the N-terminus is protonated. In the absence of water, both experimental work and calculations suggest that isolated neutral amino acids such as glycine[19−21] alanine,[22,23] valine,[24,25] and arginine [26,27] exist in the nonzwitterionic form, although for arginine these two forms of the molecule are within a few

[†] Ecole Polytechnique Fédérale de Lausanne.
[‡] University of California, Berkeley.

(1) Robertson, E. G.; Hockridge, M. R.; Jelfs, P. D.; Simons, J. P. *Phys. Chem. Chem. Phys.* **2001**, *3*, 786−795.
(2) Zwier, T. S. *J. Phys. Chem. A* **2001**, *105*, 8827−8839.
(3) Snoek, L. C.; Kroemer, R. T.; Simons, J. P. *Phys. Chem. Chem. Phys.* **2002**, *4*, 2130−2139.
(4) Simons, J. P. *C. R. Chim.* **2003**, *6*, 17−31.
(5) Carcabal, P.; Kroemer, R. T.; Snoek, L. C.; Simons, J. P.; Bakker, J. M.; Compagnon, I.; Meijer, G.; von Helden, G. *Phys. Chem. Chem. Phys.* **2004**, *6*, 4546−4552.
(6) Fricke, H.; Gerlach, A.; Unterberg, C.; Rzepecki, P.; Schrader, T.; Gerhards, M. *Phys. Chem. Chem. Phys*. **2004**, *6*, 4636−4641.
(7) Rizzo, T. R.; Park, Y. D.; Peteanu, L. A.; Levy, D. H. *J. Chem. Phys* **1985**, *83*, 4819−4820.
(8) Fye, J. L.; Woenckhaus, J.; Jarrold, M. F. *J. Am. Chem. Soc.* **1998**, *120*, 1327−1328.
(9) Jarrold, M. F. *Annu. Rev. Phys. Chem.* **2000**, *51*, 179−207.
(10) Katta, V.; Chait, B. T. *Rapid Commun. Mass Spectrom.* **1991**, *5*, 214−217.
(11) Kim, K. Y.; Chang, H. C.; Lee, Y. T.; Cho, U. I.; Boo, D. W. *J. Phys. Chem. A* **2003**, *107*, 5007−5013.
(12) Klassen, J. S.; Blades, A. T.; Kebarle, P. *J. Phys. Chem*. **1995**, *99*, 15509−15517.
(13) Kohtani, M.; Jarrold, M. F. *J. Am. Chem. Soc.* **2002**, *124*, 11148−11158.
(14) Lee, S. W.; Freivogel, P.; Schindler, T.; Beauchamp, J. L. *J. Am. Chem. Soc.* **1998**, *120*, 11758−11765.
(15) Rodriguez-Cruz, S. E.; Klassen, J. S.; Williams, E. R. *J. Am. Soc. Mass Spectrom.* **1999**, *10*, 958−968.
(16) Rodriguez-Cruz, S. E.; Klassen, J. S.; Williams, E. R. *J. Am. Soc. Mass Spectrom.* **1997**, *8*, 565−568.
(17) Wyttenbach, T.; Liu, D.; Bowers, M. T. *Int. J. Mass Spectrom.* **2005**, *240*, 221−232.
(18) Zhan, D.; Rosell, J.; Fenn, J. B. *J. Am. Soc. Mass Spectrom.* **1998**, *9*, 1241−1247.
(19) Jensen, J. H.; Gordon, M. S. *J. Am. Chem. Soc.* **1991**, *113*, 7917−7924.
(20) Iijima, K.; Tanaka, K.; Onuma, S. *J. Mol. Struct.* **1991**, *246*, 257−266.
(21) Stepanian, S. G.; Reva, I. D.; Radchenko, E. D.; Rosado, M. T. S.; Duarte, M. L. T. S.; Fausto, R.; Adamowicz, L. *J. Phys. Chem. A* **1998**, *102*, 1041−1054.
(22) Stepanian, S. G.; Reva, I. D.; Radchenko, E. D.; Adamowicz, L. *J. Phys. Chem. A* **1998**, *102*, 4623−4629.
(23) Blanco, S.; Lesarri, A.; Lopez, J. C.; Alonso, J. L. *J. Am. Chem. Soc.* **2004**, *126*, 11675−11683.
(24) Stepanian, S. G.; Reva, I. D.; Radchenko, E. D.; Adamowicz, L. *J. Phys. Chem. A* **1999**, *103*, 4404−4412.
(25) Lesarri, A.; Cocinero, E. J.; López, J. C.; Alonso, J. L. *Angew. Chem., Int. Ed.* **2004**, *43*, 605−610.
(26) Rak, J.; Skurski, P.; Simons, J.; Gutowski, M. *J. Am. Chem. Soc.* **2001**, *123*, 11695−11707.

kcal/mol in energy.[26,28] Determining the number of water molecules necessary to stabilize the zwitterionic form[3,5,29] would provide an important test of theoretical predictions.

A closely related subject is the role of salt bridges, in which the presence of another charge, either from the same molecule or an external ion, stabilizes zwitterion formation. Electrostatic interactions between amino acids (and related molecules) and a metal ion have been investigated theoretically[30−33] and experimentally by blackbody infrared radiative dissociation (BIRD),[34−38] ion mobility,[39] kinetic methods,[40,41] and vibrational photofragment spectroscopy using a free electron laser.[42] The combined effect of metal ion binding and hydration has also been investigated by collision-induced dissociation (CID)[43,44] and BIRD experiments[34,36,37] as well as theoretical calculations.[33] In an extensive set of studies, Williams and co-workers measured the dissociation rates and water binding energies of hydrated valine−cation clusters[35−37] and compared them with model compounds known to exist in either zwitterionic or nonzwitterionic structures and theoretical calculations. Although their data clearly showed a change in structure upon addition of a third water molecule to the lithiated cluster, it was not possible to determine unambiguously the number of water molecules necessary to stabilize the zwitterionic form versus the nonzwitterionic form for valine.

Another approach to investigate zwitterion formation would be to perform spectroscopic studies of the relevant species.[42] We recently developed a tandem quadrupole mass spectrometer equipped with a nanospray source for spectroscopic studies of biological ions. In the case of amino acid−metal ion water complexes, we use IR laser photofragment spectroscopy to probe the protonation/deprotonation by measuring changes in the N−H and O−H stretches that would occur upon zwitterion formation. By sequential hydration, we seek to identify the number of water molecules necessary to make the zwitterion become the minimum energy structure in the hydrated complex. We report here the results of our experiments, performed in Lausanne, together with calculations of structures and spectra carried out at Berkeley. We focused our efforts on the lithiated valine−water complexes, Val·Li$^+$(H$_2$O)$_{n=1-4}$, since these have been most extensively studied in the Williams group both by BIRD and by theory[34,35,37] and their protonated analogues, Val·H$^+$(H$_2$O)$_{n=1-4}$, as these provide insight on the assignments.

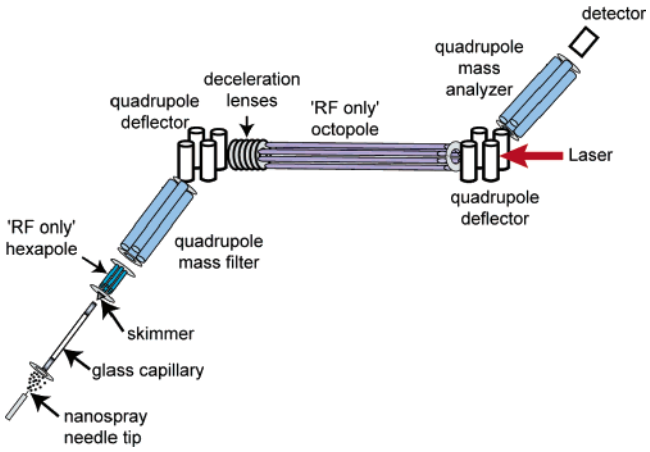

Figure 1. Schematic of ion photofragment spectrometer.

II. Experimental Approach

The experiments were performed in a home-built ion photofragment spectrometer, shown schematically in Figure 1. The details of this machine will be described more fully in a subsequent publication; we describe here only the most salient features.

Solvated lithium−valine adducts, Val·Li$^+$(H$_2$O)$_{n=1-4}$, and their protonated analogues, Val·H$^+$(H$_2$O)$_{n=1-4}$, are continuously produced at atmospheric pressure by a nanospray source (Proxeon Biosystems, DK), using a solution of 1.0 mM amino acid and 1 mM of lithium ion in deionized water. They are introduced into the vacuum system through a glass capillary and subsequently focused and accumulated in a radio frequency hexapole ion trap prior to mass analysis. Trapping in the hexapole narrows the energy distribution of ions and converts the continuous nanospray into a pulsed source that matches the duty cycle of our lasers. The pulse of ions released from the hexapole trap extends about 600 μs fwhm in duration.

A quadrupole mass filter selects a specific mass from the distribution of water clusters, and the mass-selected parent ions are deflected 90° by an electrostatic quadrupole bender, decelerated, and then refocused by electrostatic lenses into a radio frequency octopole ion guide, where a pulsed IR laser beam counterpropagates along the axis and photodissociates the cluster of interest by boiling off one water molecule. The product ion signal is deflected 90° from the laser path by a second electrostatic quadrupole and mass-resolved in a second quadrupole mass analyzer. Ions are detected using a pulse-counting Channeltron electron multiplier with a conversion dynode. The resulting signal is amplified and sent to a gated photon counter, which is interfaced to a PC via Labview. The octopole and analyzing quadrupole are kept at a pressure of $\sim 10^{-9}$ mbar during an experiment, eliminating the possibility of collision-induced dissociation.

Tunable IR laser radiation in the 2900−3800 cm^{-1} region is used to excite the parent Val·X$^+$(H$_2$O)$_n$ clusters (X = H or Li) in the octopole ion guide. In the absence of laser light, there is a small amount of thermally induced unimolecular dissociation, Val·X$^+$(H$_2$O)$_n$ → Val·X$^+$(H$_2$O)$_{n-1}$ + H$_2$O, indicating that the clusters have some internal vibrational energy. The addition of one infrared photon greatly enhances the dissociation rate, and this allows us to generate a vibrational action spectrum by collecting the mass-analyzed Val·X$^+$(H$_2$O)$_{n-1}$ fragment ion signal as a function of the infrared laser frequency. It is difficult to estimate the internal energy of the clusters, because there are two ways in which they may be formed: by evaporation of larger clusters produced by the nanospray process or by condensation of solvent vapor

(27) Chapo, C. J.; Paul, J. B.; Provencal, R. A.; Roth, K.; Saykally, R. J. *J. Am. Chem. Soc.* **1998**, *120*, 12956−12957.
(28) Price, W. D.; Jockusch, R. A.; Williams, E. R. *J. Am. Chem. Soc.* **1997**, *119*, 11988−11989.
(29) Snoek, L. C.; Robertson, E. G.; Kroemer, R. T.; Simons, J. P. *Chem. Phys. Lett.* **2000**, *321*, 49−56.
(30) Hoyau, S.; Ohanessian, G. *C. R. Acad. Sci., Ser. IIc* **1998**, *1*, 795−799.
(31) Shoeib, T.; Rodriquez, C. F.; Siu, K. W. M.; Hopkinson, A. C. *Phys. Chem. Chem. Phys.* **2001**, *3*, 853−861.
(32) Shoeib, T.; Siu, K. W. M.; Hopkinson, A. C. *J. Phys. Chem. A* **2002**, *106*, 6121−6128.
(33) Ai, H.; Bu, Y.; Han, K. *J. Chem. Phys.* **2003**, *118*, 10973−10985.
(34) Jockusch, R. A.; Lemoff, A. S.; Williams, E. R. *J. Am. Chem. Soc.* **2001**, *123*, 12255−12265.
(35) Jockusch, R. A.; Lemoff, A. S.; Williams, E. R. *J. Phys. Chem. A* **2001**, *105*, 10929−10942.
(36) Lemoff, A. S.; Bush, M. F.; Williams, E. R. *J. Am. Chem. Soc.* **2003**, *125*, 13576−13584.
(37) Lemoff, A. S.; Williams, E. R. *J. Am. Soc. Mass Spectrom.* **2004**, *15*, 1014−1024.
(38) Lemoff, A. S.; Bush, M. F.; Williams, E. R. *J. Phys. Chem.* **2005**, *109*, 1903−1910.
(39) Wyttenbach, T.; Witt, M.; Bowers, M. T. *J. Am. Chem. Soc.* **2000**, *122*, 3458−3464.
(40) Talley, J. M.; Cerda, B. A.; Ohanessian, G.; Wesdemiotis, C. *Chem.*—Eur. J. **2002**, *8*, 1377−1388.
(41) Kish, M. M.; Ohanessian, G.; Wesdemiotis, C. *Int. J. Mass Spectrom.* **2003**, *227*, 509−524.
(42) Kapota, C.; Lemaire, J.; Maitre, P.; Ohanessian, G. *J. Am. Chem. Soc.* **2004**, *126*, 1836−1842.
(43) Rodgers, M. T.; Armentrout, P. B. *Acc. Chem. Res.* **2004**, *37*, 989−998.
(44) Ye, S. J.; Moision, R. M.; Armentrout, P. B. *Int. J. Mass Spectrom.* **2005**, *240*, 233−248.

on the bare amino acid ions in the mild supersonic expansion emanating from the glass capillary.[15] Moreover, clusters are almost certainly warmed in the collection hexapole, where they experience collisions during storage. Threshold dissociation energies calculated by Lemoff and Williams[37] for the lithiated valine−water clusters range from 0.88 eV for the $n = 1$ species to 0.5 eV for the $n = 3$ species—all greater than the energy of a single infrared photon in the light−atom stretch region, and we verified that the fragmentation signal is linear with laser power. This means that the species that we study must have a significant amount of thermal energy to be able to dissociate upon IR excitation.

We generate IR excitation pulses of energy up to 6 mJ/pulse near 3 μm by a two-stage difference frequency mixing (DFM) setup. The second-harmonic output of a single-mode Nd:YAG laser pumps a dye laser, which generates tunable visible radiation between 629 and 666 nm using DCM laser dye. The 1064 nm fundamental of the same Nd:YAG laser passes through a $\lambda/2$ plate and a polarizing beam splitter, which produces linearly polarized beams of 150 mJ/pulse p-polarized light and 300−400 mJ/pulse s-polarized light. The output of the dye laser is combined with the former on a CaF_2 dichroic mirror and sent through a $LiNbO_3$ crystal for difference frequency mixing. The crystal is installed in an Inrad Autotracker II for phase matching during the laser scan, allowing for continuous tuning of the IR frequency. The resulting 4−5 mJ/pulse near 1.6 μm emerging from this DFM stage is separated from the 1064 nm pump beam by a CaF_2 dichroic mirror, while the residual visible light is absorbed on a silicon plate. The remaining 300−400 mJ of the Nd:YAG fundamental is combined with the 1.6 μm beam on an infrared fused silica dichroic mirror for a second stage difference frequency mixing using two 25 mm long $KTiOPO_4$ (KTP) crystals arranged in a walkoff-compensated configuration and stabilized against temperature drifts induced by the pump beam. This second DFM stage generates up to 6 mJ/pulse of idler around 3 μm. The KTP crystals allow tuning of the infrared frequency from 3300 to 3800 cm^{-1}, while a pair of KTA ($KTiAsO_4$) crystals provides access to lower frequencies (2900−3300 cm^{-1}). The residual 1064 nm pumping radiation is separated from the s-polarized 3 μm beam using a CaF_2 dichroic mirror, and a pair of silicon plates at the Brewster angle reflect the remainder 1.6 μm beam. The p-polarized 3 μm radiation is then directed into the octopole ion guide through a BaF_2 window mounted at the Brewster angle.

An eight-channel pulse delay generator handles synchronization between the dumping of the hexapole ion trap, laser firing, ion counting, and data acquisition. A Labview program controls communications with a data acquisition card (National Instruments PCI-6110 S), steps the dye laser wavelength, rotates the second-stage DFM stage crystals, and retrieves data from the gated photon counter. Instrument control and data acquisition of laser-on and laser-off signals are operated through GPIB interfaces.

L-Valine (Val) and L-tryptophan (Trp) were purchased from Sigma-Aldrich Co. (Switzerland), and lithium chloride was obtained from AppliChem GmbH (Germany).

III. Computational Details

Geometries for the low-energy structures of Val·Li+$(H_2O)_{1-2}$ have been reported previously.[37] Candidate low-energy structures of Val·$Li^+(H_2O)_3$ and Val·$H^+(H_2O)_{1-3}$ were determined using a combination of conformational searching and chemical intuition. Initial structures for these clusters were generated using Monte Carlo conformation searching with the MMFF94 force field using Macromodel 8.1 (Schrodinger, Inc., Portland, OR). For the initial search, no constraints were placed on the molecules, and at least 10 000 conformations were generated. In these simulations, the significant hydrogen-bonding motifs were identified within the first several thousand conformations generated. In the case of Val·$Li^+(H_2O)_3$, separate searches were performed for the nonzwitterionic cluster and the zwitterionic cluster in which the amine nitrogen is protonated and the carboxylic acid deprotonated. For Val·$H^+(H_2O)$, the amine nitrogen and carbonyl oxygen were each evaluated as potential protonation sites. In addition, a salt bridge containing cluster with a protonated amine, a deprotonated carboxylic acid, and a hydronium was considered. In subsequent quantum mechanical calculations, all structures within 30 kJ/mol of the lowest energy structure minimized to form without a salt bridge and with the amine group protonated. On the basis of these results, the amino acid in Val·$H^+(H_2O)_{2-3}$ was assumed to adopt a structure with a protonated amine and a neutral carboxylic acid group. Additional candidate structures were generated by altering structures found in the Monte Carlo simulations by incorporating an additional water molecule or changing the cis/trans conformation of the carboxylic acid.

After identifying low-energy structures, hybrid method density functional calculations (B3LYP) were performed using Jaguar v. 5.5 (Schrodinger, Inc., Portland, OR) with the 6-31G* basis set. Final geometries were then obtained by subsequent minimization using the 6-31++G** basis set. Vibrational frequencies and intensities were calculated using numerical derivatives of the B3LYP/6-31++G** energy-minimized Hessian. A constant scale factor of 0.956 was applied to all calculated frequencies in all spectra to account for anharmonicity and other factors. This single scale factor was obtained by an approximate best fit to all measured spectra. It is important to note that because the spectra are calculated in the "double-harmonic" approximation (i.e., linear dipole moment function and harmonic vibrations), the calculated results will not predict any overtone vibrations. A few notes of caution are in order regarding the comparison of experiment and theory. Because of the well-known problem with DFT calculations in treating dispersion interactions, one should be increasingly suspicious of the structure predictions with increasing cluster size. In general, one should not make too much distinction between two species that have energies within a few kJ/mol. Also, depending on the mechanism of cluster formation, the barriers separating different conformers, and their internal energy, several different conformers of a given species may be present in the ion beam, and this possibility should be noted when comparing experiment and theory. Another important point is that our experiment measures an "action spectrum" (i.e., a spectrum of those clusters that absorb and dissociate on a sufficiently short time scale), while what we calculate is an absorption spectrum. If excitation of different vibrational modes were to lead to different dissociation rates, this would show up as a skewing of intensities that we observe. It is also possible that energy threshold effects could skew the intensities across a spectrum, since the dissociation rate will increase with increasing energy and we observe only the dissociation fragments that have occurred within ~300 μs flight time through the octopole. One must therefore be careful to not draw excessively detailed conclusions from spectral intensities.

We use the following nomenclature for calculated cluster conformations: a first letter (H or L) to distinguish protonated and lithiated clusters followed by a number (indicating the number of water molecules) and a letter (A, B, C, etc.) to distinguish different conformations of the same cluster. Thus, H1•A would be a calculated conformation of monohydrated, protonated valine, while L3•C would be that of a lithiated valine cluster with three water molecules.

IV. Spectroscopic Results and Calculations

We adopt certain notation conventions to characterize the bonding properties of solvent molecules and the amino acid isomers. Depending on the hydrogen-bonding motif we use the convention of "donor" if the water molecule donates the hydrogen atom and "acceptor" when the interaction involves the free lone pair of the oxygen atom. Hence, we label in parentheses a single-acceptor water molecule (A), a single donor (D), a double-acceptor (AA), and a single-acceptor−single-donor (AD).

The following definitions characterize the amino acid conformation based on the orientation of the amino group (NH_2 or

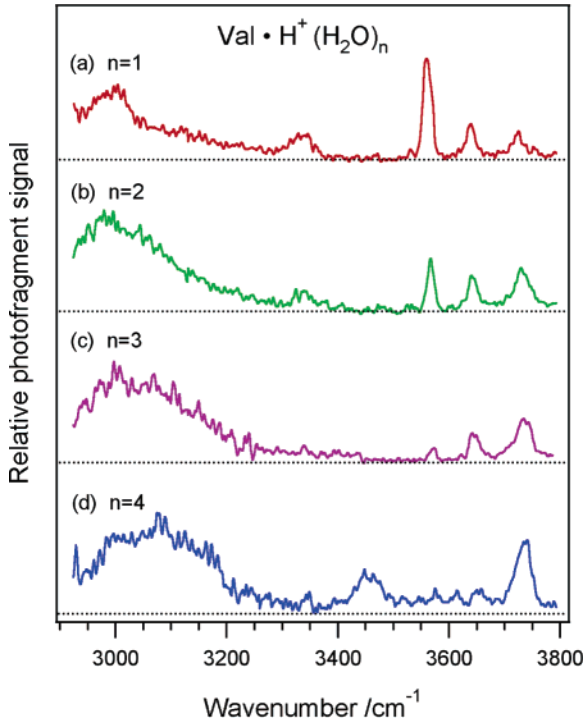

Figure 2. Infrared photofragment spectra of Val·$H^+(H_2O)_{n=1-4}$.

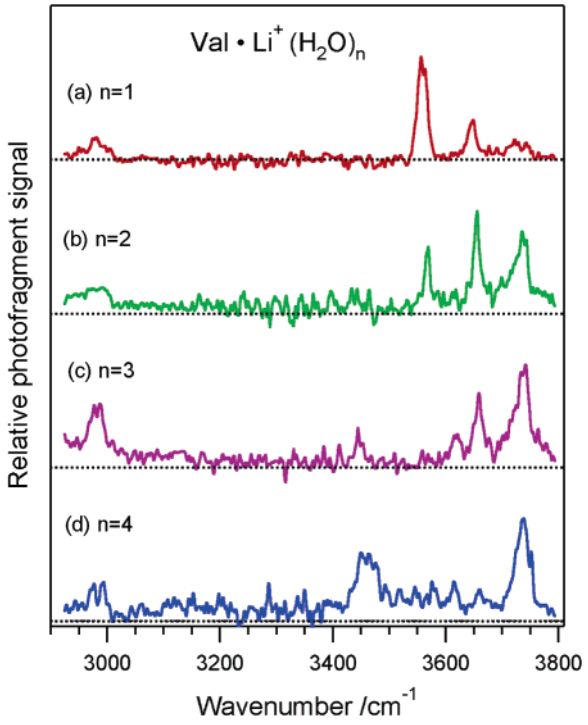

Figure 3. Infrared photofragment spectra of Val·$Li^+(H_2O)_{n=1-4}$.

NH_3^+) relative to the carboxylic group (COO−H). We refer to a syn conformer if the amino group faces the carbonyl oxygen of COOH and an anti conformer if it faces the O−H of COOH after rotation of the carboxylic group about the C−C^α bond. Moreover, we adopt the abbreviations NZ to describe a charge-solvated structure in which the amino acid is in its neutral (i.e., nonzwitterionic) form, whereas Z stands for a salt-bridge structure where the amino acid is a zwitterion.

In lithiated water clusters we distinguish different structures based on the coordination site of the lithium cation. An "NO-coordinated" structure denotes Li^+ bonded between the nitrogen atom of the amino group and the carbonyl oxygen of the C-terminus, whereas "OO coordination" indicates binding of the lithium cation between the oxygen atoms of the carboxylic acid.

It is important to note that our spectroscopic technique is not conformer-specific, and thus it is possible, and even likely, that more than one conformer of the hydrated valine clusters contributes to each infrared spectrum.

Infrared photofragmentation action spectra obtained for Val·$H^+(H_2O)_{n=1-4}$ in the region 2900−3800 cm^{-1} are shown in Figure 2 and those for Val·$Li^+(H_2O)_{n=1-4}$ in Figure 3. Our general approach to interpreting these spectra is as follows. We first assign the major features of each spectrum by comparison with the IR spectra of isolated gas-phase valine,[24] hydrated alkali metal ion clusters, [45,46] protonated amine water clusters,[11,47] as well as hydrated clusters of other protonated amino acids measured in our laboratory. We then compare assigned spectra to those calculated for low-energy structures of the corresponding species to identify likely conformations. In making such a comparison, it is important to remember that that there may be more than one stable conformer formed for a given cluster size, each of which would contribute to a particular spectrum.

At first glance it is worth noting that although these two families of clusters are different species with a completely different charge carrier, their spectra show remarkable similarities in the high-frequency portion of the corresponding spectra. We discuss in detail below both the similarities and differences in the spectra of these two cluster families and the implications for understanding the solvation of these species.

A. Protonated Valine Water Clusters ValH·$^+(H_2O)_n$. The hydration process is controlled by a delicate balance of noncovalent interactions between neighboring groups within the molecule and between the molecule and its solvent environment. The isopropyl residue side chain of valine is likely to neither interact through H-bonding with water molecules nor give rise to intramolecular self-solvation of the amino acid, leaving the N-terminus and the C-terminus as the only possible sites for water attachment during microsolvation. Water may attach either to the two oxygen atoms or the hydrogen atom of the carboxylic group or to one of the three hydrogen atoms of the protonated amino group.

Protonation occurs at the amino group of valine, which removes the free lone pair of the nitrogen atom and thus limits the hydrogen-bonding mode of the N-terminus to a "donor-only" site. This should have important structural consequences, since the conformational preferences of neutral amino acids[24,48] are influenced by stabilization of the intermolecular hydrogen bond established between the free lone pair of the nitrogen and the donating proton of the carboxylic acid terminus. Moreover, the presence of the charge introduces an additional electrostatic driving force for intermolecular noncovalent interactions, especially with the water molecules.

(45) Vaden, T. D.; Weinheimer, C. J.; Lisy, J. M. *J. Chem. Phys.* **2004**, *121*, 3102−3107.
(46) Weinheimer, C. J.; Lisy, J. M. *J. Chem. Phys.* **1996**, *105*, 2938−2941.
(47) Wang, Y. S.; Chang, H. C.; Jiang, J. C.; Lin, S. H.; Lee, Y. T.; Chang, H. C. *J. Am. Chem. Soc.* **1998**, *120*, 8777−8788.
(48) Snoek, L. C.; Kroemer, R. T.; Hockridge, M. R.; Simons, J. P. *Phys. Chem. Chem. Phys.* **2001**, *3*, 1819−1826.

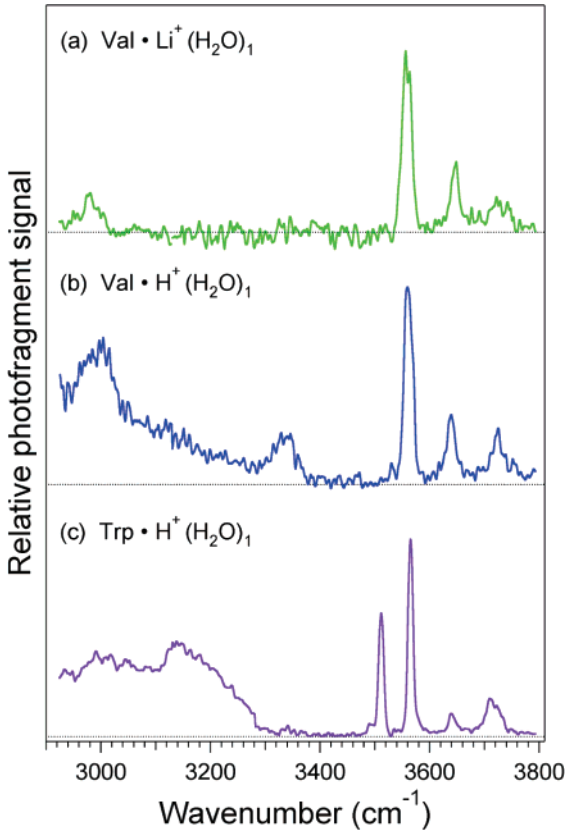

Figure 4. Comparison of infrared spectra of (a) Val·$Li^+(H_2O)$, (b) Val·$H^+(H_2O)$, and (c) Trp·$H^+(H_2O)$.

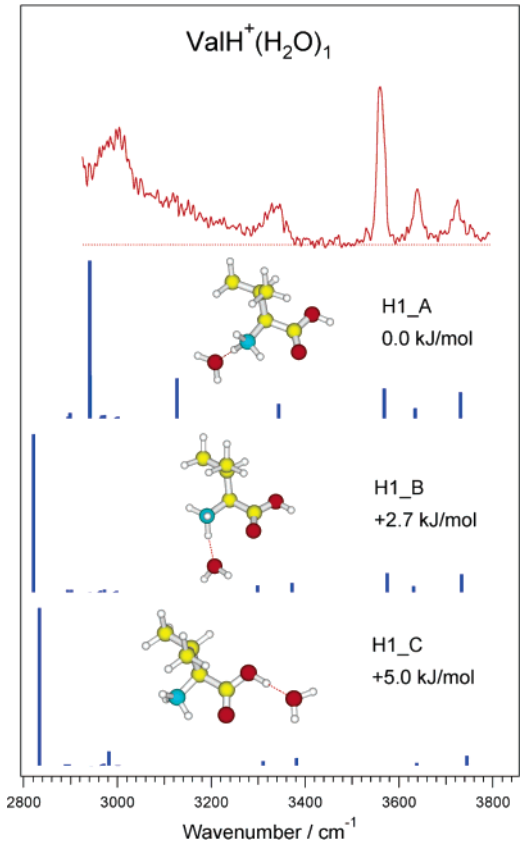

Figure 5. Comparison of measured infrared spectrum of Val·$H^+(H_2O)$ with calculated spectra corresponding to the structures shown.

(i) ValH^+·(H_2O). Three groups of transitions are visible in the spectrum of ValH^+·(H_2O): a strong absorption band at 3560 cm^{-1}, two weaker bands at 3640 and 3725 cm^{-1}, and some broader features below 3400 cm^{-1}. We make preliminary spectral assignments by comparison with spectroscopic results of analogous chemical compounds, either obtained experimentally in our lab or available in the literature. As shown in Figure 4, the three highest frequency bands are also present in the ValLi^+·(H_2O) and TrpH^+·(H_2O) spectra, which suggests that they arise from vibrations common to these clusters: two water O−H stretches, the carboxylic acid O−H stretch, and the N−H stretches of the amino group. To identify unambiguously which of these three common features belongs to the carboxylic acid O−H stretch, we also measured the IR spectrum of water clusters of tryptamine (not shown), a tryptophan analogue containing no carboxylic acid group: upon removal of the COOH, the 3560 cm^{-1} band disappears. We assign the bands at 3649 and 3731 cm^{-1} to free water O−H stretches. Indeed, isolated gas-phase water exhibits two bands, the symmetric O−H stretch at 3657 cm^{-1} and the antisymmetric stretch at 3756 cm^{-1}.[49] In Val·$H^+(H_2O)$ these bands are shifted to lower frequency and the symmetric stretch presents a higher IR relative intensity over the antisymmetric stretch as also reported by Lee and co-workers in the spectra of hydrated, protonated amines.[11,47] We assign the feature at 3337 cm^{-1} to non-hydrogen-bonded NH stretches, as these fall in the region observed in vibrational spectra of protonated ammonia and protonated amines,[11,50] where they appear to gain intensity compared to neutral amines.[2]

Upon forming a hydrogen bond ammonium NH stretches tend to shift to lower frequency and broaden,[47] and this can account for the broad structures below 3200 cm^{-1}, which we observe in all hydrated amino acids where we expect to have a solvated, protonated amine (see, for example, the hydrated tryptophan spectrum in Figure 4c). The CH stretch bands should appear in the region of 3000 cm^{-1}, but these are likely to be buried below the stronger hydrogen-bonded ammonium stretch bands.

While these assignments provide information about the light-atom stretch vibrations in the cluster as well as hydrogen-bonding sites, they do not provide a detailed picture of the cluster conformation. More detailed structural information can only be obtained by comparison with calculated spectra of stable conformers, as shown in Figure 5.

All lowest energy structures calculated for ValH^+·(H_2O) clusters are in a syn conformation (i.e., with the carbonyl facing the ammonium). In structures H1•A and H1•C (Figure 5) an additional stabilizing interaction occurs between the ammonium group and the carbonyl oxygen. In structure H1•B the water interacts along an N−H bond facing the carbonyl oxygen and breaks this intramolecular interaction. The major difference between H1•A and H1•C is the hydrogen-bonding site of the water, which occurs on the ammonium group in the former and the carboxylic acid OH group in the latter. It is surprising that the calculations predict only a 5 kJ/mol energy difference between these two structures, as we would expect electrostatic interactions to cause a substantially larger stabilization upon hydration of the ammonium. This can be attributed to a

(49) Herzberg, G. *Molecular Spectra and Molecular Structure II. Infrared and Raman Spectra of Polyatomic Molecules*; Van Nostrand Reinhold: New York, 1945.

(50) Macleod, N. A.; Simons, J. P. *Phys. Chem. Chem. Phys.* **2004**, *6*, 2821−2826.

significant destabilization of the amino−carboxylic oxygen interaction upon binding a water molecule to the amino group.

The observed spectrum is not consistent with that calculated for conformer H1•C, in which the COOH stretch is predicted to be red shifted beyond the region of our measured spectrum. The strong absorption observed at 3560 cm^{-1} for the free COO−H thus rules out the possibility of water binding to the carboxylic acid. Structures H1•A and H1•B correctly predict the position of the free COOH band as well as the two free water stretches and attachment of water to the ammonium group. The latter is consistent with the observed broad absorption band peaking around 3000 cm^{-1}.

Structures H1•A and H1•B differ by the orientation of the water molecule and the ammonium, which may influence the intramolecular stabilization of the ammonium charge by the carbonyl oxygen. There is good agreement between the experimental spectrum and the calculated spectrum of H1•A, while the agreement with H1•B is noticeably worse in the low-frequency part of the spectrum due to a stronger red shift of hydrogen-bonded ammonium band. Because the shift causes the band to fall out of the frequency range accessed by our experiment, we cannot eliminate the possibility of the H1•B conformer contributing to the spectrum.

(ii) ValH$^+$·(H$_2$O)$_2$. The spectrum of ValH$^+$·(H$_2$O)$_2$ (Figure 2) is similar to that of the monohydrated species. All of the bands are slightly blue shifted in the doubly hydrated species, and noticeable differences exist in the observed relative band intensities. The ValH$^+$·(H$_2$O)$_2$ spectrum is marked by a weaker absorption of the free NH stretch at 3340 cm^{-1} relative to the hydrogen-bonded NH absorption centered at ∼3020 cm^{-1}, which is broader in comparison with the spectrum of the singly hydrated species. Moreover, the free water vibrations at 3641 and 3730 cm^{-1} gain in relative intensity and become comparable to the free COO−H stretch at 3567 cm^{-1}.

As shown in Figure 6 the minimum energy structure calculated for ValH$^+$·(H$_2$O)$_2$, H2•B, exhibits (somewhat surprisingly) a hydrogen bond between the carboxylic acid OH and the second water molecule, with the first water remaining on the ammonium. The persistence of the free COO−H stretch absorption at 3567 cm^{-1} in the observed spectrum, albeit at slightly reduced relative intensity, suggests that this conformer cannot be the dominant structure, although we cannot rule out its contribution to the observed spectrum since the hydrogen-bonded COOH falls outside our spectral range.

Calculations also show evidence for a stable conformer, H2•C, where the second water molecule resides in the outer solvent shell. On the basis of the calculated vibrational frequencies of this structure, the hydrogen-bonded ammonium would be red shifted beyond our detectable frequency range while the OH bond bridging the inner- and outer-shell water molecules would give rise to a strong absorption band at 3284 cm^{-1}. While the experimental spectrum does indeed show a band near 3300 cm^{-1} which could, in principle, correspond to this shifted OH stretch, the persistence of the broad absorption around 3000 cm^{-1} in the measured spectrum and total absence of bands in this region of the calculated spectrum suggest that H2•C is not the dominant conformer.

In contrast to the conformers H2•B and H2•C discussed above, we find good agreement between the calculated IR spectrum of conformer H2•A and the experimental spectrum

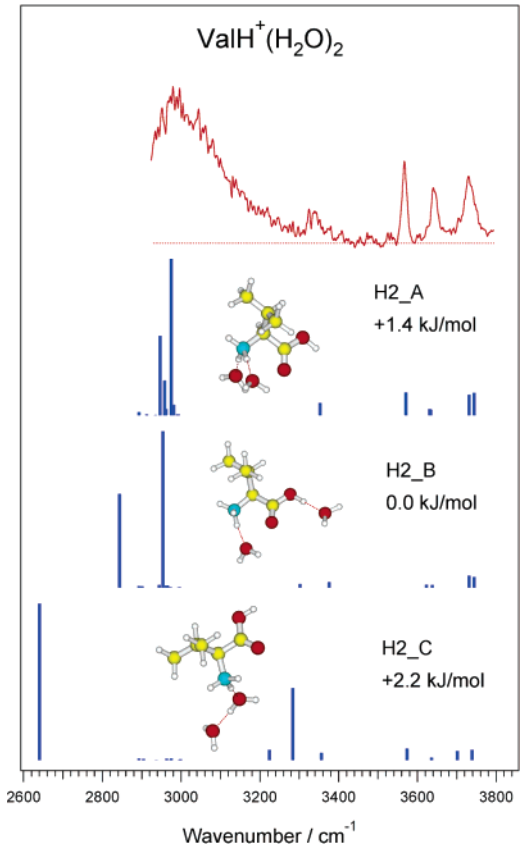

Figure 6. Comparison of measured infrared spectrum of Val·H$^+$(H$_2$O)$_2$ with calculated spectra corresponding to the structures shown.

of ValH$^+$·(H$_2$O)$_2$. The good prediction of the position of the hydrogen-bonded ammonium, slightly blue shifted in comparison with ValH$^+$·(H$_2$O), together with the decrease in intensity of the free ammonium NH stretch band over that of the hydrogen-bonded ammonium are consistent with the presence of two hydrogen-bonded NH stretches and only one free NH stretch. Moreover, the free OH stretch water bands are almost doubled in intensity relative to the free COO−H compared to ValH$^+$·(H$_2$O), which is consistent with the presence of twice the number of OH absorbing vibrations upon addition of a second water molecule. The fact that the water symmetric and antisymmetric stretch bands are close to that of free water, both in the measured spectrum and the calculated one for this conformer, indicates that neither of the water molecules acts as hydrogen-bond donors.

(iii) ValH$^+$·(H$_2$O)$_3$. The infrared spectrum of ValH$^+$·(H$_2$O)$_3$ is similar to those of the smaller water clusters, albeit with several noticeable changes. The feature assigned to the non-hydrogen-bonded ammonium decreases to the point where it is not obvious that it still appears, and the free COO−H band decreases in intensity relative to both the free water stretches and the broad hydrogen-bonded ammonium absorption. All the major features (hydrogen-bonded ammonium stretches, free COOH stretch, and free water stretches) shift slightly to the blue compared to the smaller clusters.

As shown in Figure 7 DFT calculations predict a minimum energy structure having one water hydrogen bonded to the carboxylic acid and two water molecules on the ammonium NH bonds (H3•B), whereas the other energetically competing structure (H3•C) contains two inner-shell waters on the am-

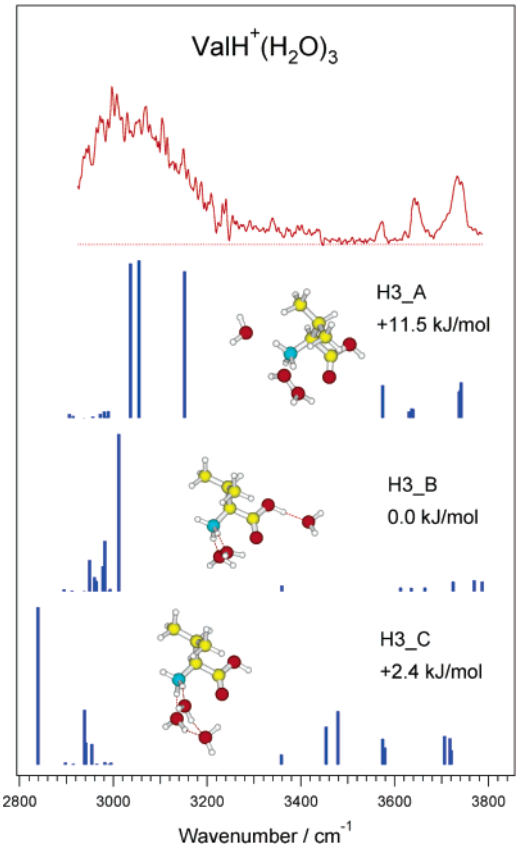

Figure 7. Comparison of measured infrared spectrum of Val·$H^+(H_2O)_3$ with calculated spectra corresponding to the structures shown.

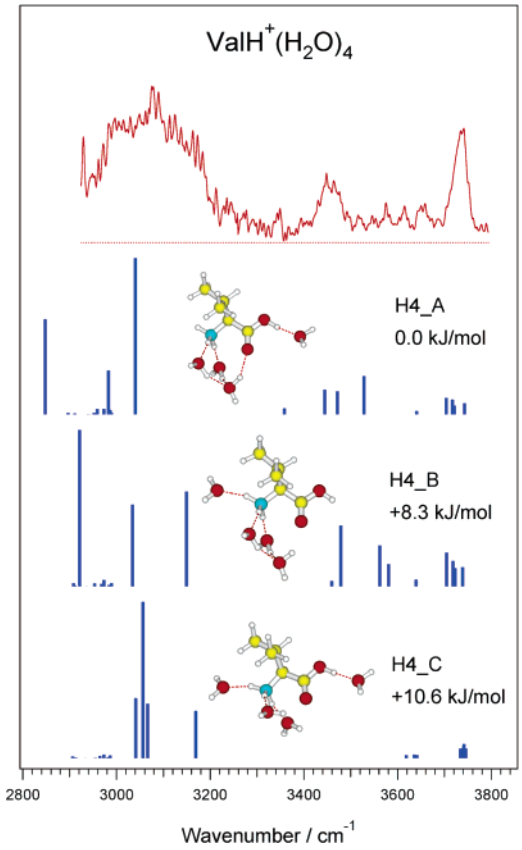

Figure 8. Comparison of measured infrared spectrum of Val·$H^+(H_2O)_4$ with calculated spectra corresponding to the structures shown.

monium and the third in the outer shell acting as a double hydrogen-bond acceptor, forming a cyclic water structure. Surprisingly, the first low-energy conformer hydrating the ammonium group with water molecules interacting with each of the NH bonds (H3•A) lies 11.5 kJ/mol higher in energy than the previously cited structures. Such an energy difference starts to be larger than the uncertainty of the calculations, suggesting that DFT predicts H3•A to be a higher energy conformer given the level of our calculation.

The free COO−H band at 3571 cm^{-1} in the measured spectrum rules out the exclusive presence of H3•B, although we cannot eliminate the possibility of a small contribution from this conformer. The calculated vibrational spectrum of H3•C exhibits characteristic absorptions of the H-bonded water OH stretches around 3500 cm^{-1}, which do not appear in the experimental spectrum. Moreover, the cyclic water structure would show a substantial red shift of the H-bonded ammonium bands below 3000 cm^{-1}, which is not observed. Taken together, this allows us to rule out the contribution of such a conformer to our spectrum.

The spectrum of the higher energy conformer predicted by DFT (H3•A) seems to agree best with the experimental data. It reproduces well the free COOH band at 3571 cm^{-1} and is consistent with the relative increase in intensity of the hydrogen-bonded ammonium bands and the free water bands that come with the increase in the number of oscillators.

(iv) $ValH^+\cdot(H_2O)_4$. While the infrared spectrum of $ValH^+\cdot(H_2O)_4$ (Figure 8) continues the general trend established by the smaller clusters (i.e., decreasing intensity of the carboxylic acid stretch, increasing intensity of the higher-frequency water stretch, and persistence of the broad, hydrogen-bonded ammonium band), some new bands begin to appear. A completely new feature appears at 3456 cm^{-1}, and a series of smaller peaks seems to grow in to its high-frequency side.

There are two things that seem clear from the measured IR spectrum: (1) the characteristic broad feature between 3000 and 3200 cm^{-1} implies that at least some of the water molecules remain attached to the ammonium group and (2) the strong enhancement of the higher frequency free OH stretch band suggests that most of the water molecules have at least one donor hydrogen bond and one free OH stretch, the former being strongly shifted to lower wavenumber while the latter appears near the asymmetric stretch frequency of free water. It is difficult to draw any further conclusions from the observed spectrum without the help of calculations.

In lieu of performing an exhaustive conformational sampling of $ValH^+\cdot(H_2O)_4$, we use our chemical intuition and calculate vibrational spectra of three candidate conformers based on the extensive search accomplished for $ValH^+\cdot(H_2O)_3$. Starting from the dominant conformer H3•A of the trihydrated molecule, we add one water molecule near the carboxylic group to obtain a structure with all the available amino acid sites fully hydrated, shown as H4•C in the bottom panel of Figure 8. Another logical starting point for stable structures of $ValH^+\cdot(H_2O)_4$ is the conformer H3•C of the trihydrate, since this already contains water molecules that donate a hydrogen bond. We explore two conformers with H3•C parentage—one in which the additional water binds to the remaining free ammonium NH (H4•B) and the other to the carboxylic acid OH (H4•A). The relative energies of the three calculated structures are shown in Figure 8.

The calculated spectrum of the conformer H4•C is clearly not consistent with its being the dominant conformer contributing to the measured spectrum, since no spectral features are predicted between 3200 and 3600 cm^{-1}. On the other hand, conformers H4•A and H4•B, which both contain cyclic water clusters, clearly show peaks in this region arising from water molecules that simultaneously donate and accept hydrogen bonds (AD). In addition, these structures show a strong high-frequency OH band arising from the dangling water OH bonds. While the calculated spectrum of H4•B shows better general agreement with the experimental data than H4•A, we cannot clearly distinguish between them. Moreover, because we have not performed an exhaustive search of the conformational space, we cannot rule out the existence of other structures that would be consistent with the measured spectrum. In particular, we cannot eliminate the possible existence of structural isomers where the cyclic water cluster is broken and the outer-shell water molecule interacts as an AD with one another in the inner shell rather than as an AA.

B. Lithiated Valine−Water Clusters ValLi$^+$·$(H_2O)_n$. The properties of lithiated valine water clusters should be intrinsically different from those of the corresponding protonated species. In lithiated valine the amino acid appears in its neutral form and the hydrated cluster of the amino acid derives its charge through coordination to the lithium ion. The neutral form of valine offers different possible sites for noncovalent interactions: the NH_2 group and the carboxylic OH may act both as a hydrogen-bond donor and acceptor and the carbonyl oxygen as an acceptor. In addition, the lithium ion will play a major role in determining the arrangement of solvent, both by occupying potential hydrogen-bonding sites on the valine backbone and by directly binding water molecules. Thus, the lithium ion and the amino acid compete as potential solvation sites. The coordination number of lithium in gas-phase water clusters is generally four,[51−54] with the water molecules forming a tetrahedral structure around the metal ion in the first solvent shell. The attraction between the electronegative oxygen atoms of water and the lithium cation is about 1 order of magnitude stronger than hydrogen bonding between water molecules,[52] which would suggest that the first few water molecules added to lithiated valine will likely hydrate the alkali ion rather than a site on the amino acid or build up a second solvent shell.

(i) ValLi$^+$·(H_2O). The high-frequency region of the ValLi$^+$·(H_2O) spectrum (Figure 3) shows a strong resemblance to that of the corresponding protonated species: it exhibits a strong absorption band at 3560 cm^{-1}, characteristic of a free carboxylic acid OH stretch, and two less intense peaks at 3649 and 3731 cm^{-1}, characteristic of symmetric and antisymmetric OH stretches in the free water molecule. The only absorption that appears below 3500 cm^{-1} is a small band at 2979 cm^{-1}.

As in ValH$^+$·(H_2O) water clusters, the symmetric and antisymmetric water bands of Val·Li$^+$$(H_2O)$ appear lower in frequency than in a free water molecule, with the lower frequency symmetric stretch band being the more intense one. Similar spectroscopic signatures have been observed by Lisy and co-workers in the vibrational spectra of alkali ion water clusters[45] and were attributed to the electrostatic interaction between the lithium cation and water. This would suggest that the water is preferentially solvating the charge.

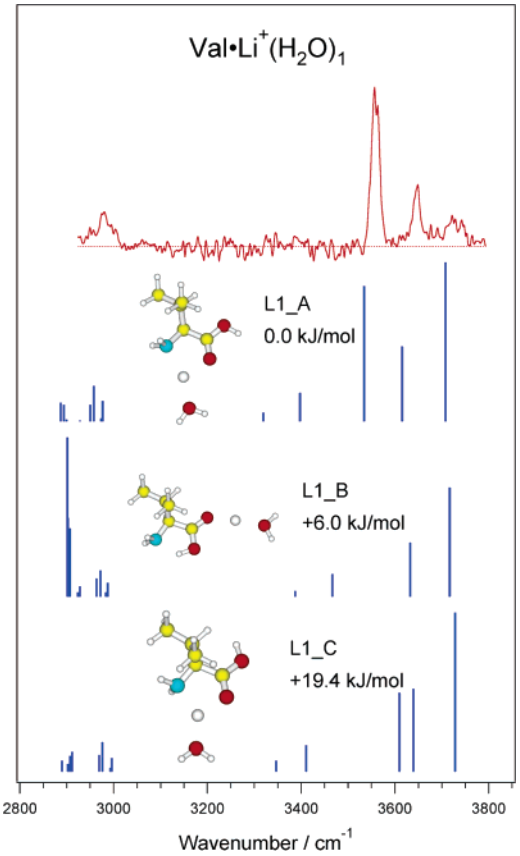

Figure 9. Comparison of measured infrared spectrum of Val·Li$^+$$(H_2O)_1$ with calculated spectra corresponding to the structures shown.

There seems to be no evidence in our spectra for the presence of either free N−H stretch bands, which would be expected to occur in the region 3200−3400 cm^{-1} based on the spectrum of neutral valine,[24] or hydrogen-bonded ammonium bands, which we observed in the protonated clusters in the region 3000−3200 cm^{-1}. The former is not surprising since the symmetric and antisymmetric stretch vibrations of the neutral amino group are known to be extremely weak.[55] The latter combined with the carboxylic OH stretch band at 3560 cm^{-1} suggests that valine does not exist in the zwitterionic form. The remaining band at 2979 cm^{-1} is likely to arise from CH stretch absorptions, which are hidden beneath the hydrogen-bonded ammonium bands in the protonated species.

We show representative calculated structures of ValLi$^+$·(H_2O) in Figure 9. The calculated frequencies of the lowest energy conformer, L1•A, show good agreement with the measured spectrum. In this cluster the lithium is coordinated between the carbonyl oxygen and the amino nitrogen (NO coordinated), which is likely to stabilize the syn conformation of valine, and the water molecule solvates the lithium ion. This shows the predominance of electrostatic forces between the water dipole and the cation in the first step of hydration. L1•C is a higher energy conformer also with an NO-coordinated lithium but differs from L1•A by the carboxylic OH bond in the trans

(51) Loeffler, H. H.; Rode, B. M. *J. Chem. Phys.* **2002**, *117*, 110−117.
(52) Lyubartsev, A. P.; Laasonen, K.; Laaksonen, A. *J. Chem. Phys.* **2001**, *114*, 3120−3126.
(53) Dzidic, I.; Kebarle, P. *J. Phys. Chem.* **1970**, *74*, 1466−1474.
(54) Rodgers, M. T.; Armentrout, P. B. *J. Phys. Chem. A* **1997**, *101*, 2614−2625.
(55) Carney, J. R.; Zwier, T. S. *J. Phys. Chem. A* **2000**, *104*, 8677−8688.

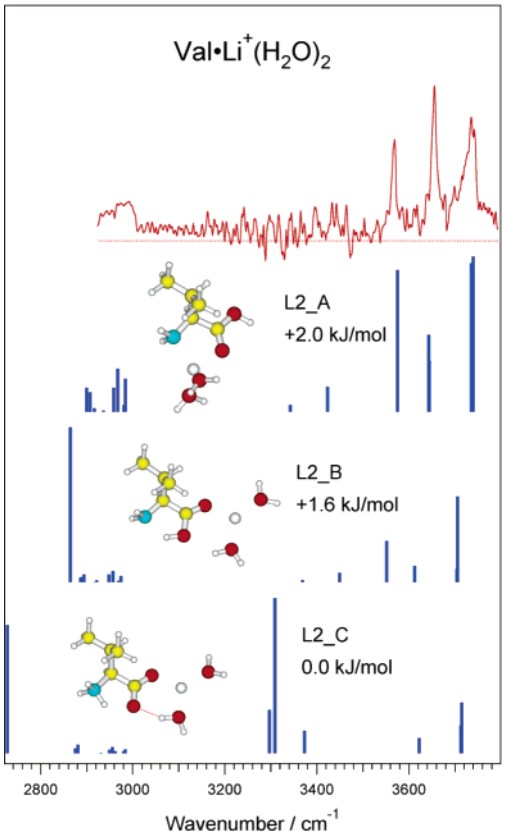

Figure 10. Comparison of measured infrared spectrum of Val·$Li^+(H_2O)_2$ with calculated spectra corresponding to the structures shown.

position with respect to the carbonyl. This structural difference gives rise to a blue shift of the corresponding absorption band above 3600 cm^{-1}, which is not visible in our spectra, eliminating this conformer from our consideration.

L1•B is a representative conformation of OO-coordinated structures, with the lithium cation bound to the carboxylic group and the valine adopting an anti conformation stabilized through intramolecular hydrogen bonding between the carboxylic OH and the amino group. The latter shifts the COO−H stretch to the red edge of the spectrum, below 2900 cm^{-1}, making it inconsistent with the measured spectrum, which shows clear evidence for a COO−H stretch absorption at 3560 cm^{-1}. It follows that valine is not present in its zwitterionic form in $ValLi^+•(H_2O)$ since this would imply the disappearance of the COO−H vibration.

(ii) $ValLi^+•(H_2O)_2$. The spectrum of Val·$Li^+(H_2O)_2$ is similar to that of Val·$Li^+(H_2O)$—it exhibits bands at 3656 and 3738 cm^{-1}, slightly blue shifted from the previously assigned free water O−H bands in Val·$Li^+(H_2O)$. In place of the typically strong COO−H vibration there appears a weaker and blue-shifted band at 3569 cm^{-1}. While this may be interpreted as the carboxylic acid OH stretch, as discussed below, it is also possible that this arises from a weakly hydrogen-bonded OH water stretch. It is difficult to assign this band without the help of calculated spectra, which we show in Figure 10.

Calculations predict that the lowest energy structure (L2•C) of Val·$Li^+(H_2O)_2$ has valine in the zwitterionic form. In this structure the carboxylic acid proton resides on the amino group and the lithium cation is solvated by the carboxylate group, forming a salt bridge with the zwitterion. In this OO-coordinated structure one of the water molecules exclusively solvates the metal ion whereas the second water establishes a hydrogen bond with one oxygen of the carboxylate, resulting in a substantial red shift of the water O−H vibration to about 3300 cm^{-1}. The vibrational band appearing at 3569 cm^{-1} in the observed spectrum, indicative of a free COO−H stretch, together with the lack of spectral features observed in the region 3300−3400 cm^{-1} seems to rule out the existence of an OO-coordinated zwitterionic structure.

The energetically competitive nonzwitterionic (NZ) OO-coordinated structure (L2•B) differs from the zwitterionic form (L2•C) only by the position of the proton on the carboxylic group characteristic of the neutral form. This minor difference substantially affects the appearance of the spectrum. The donating water hydrogen bond orients the proton of the carboxylic acid toward the amino group, which favors an intramolecular hydrogen-bonded bridge HOH→O−H(COO−H)→ NH_2. Such a geometry gives rise to a H-bonded O−H vibration of the donor water around 3600 cm^{-1} and a red shift of the COO−H to 2864 cm^{-1}. The experimental spectrum of $ValLi^+•(H_2O)_2$ cannot rule out the presence of such a structure: the band at 3570 cm^{-1} previously assigned to a free COO−H stretch could be assigned here to the hydrogen-bonded OH of water. The lack of data below 2900 cm^{-1} does not allow us observe an intramolecular hydrogen-bonded COO−H band, although the broadening of the band around 3000 cm^{-1} might suggest the beginning of such a band.

The NO-coordinated cluster (L2•A) has a similar structure to the most stable conformer of the monohydrated cluster, with a second water molecule bound to the lithium cation, providing a four-coordinate shell around the ion. The calculated spectrum corresponding to this structure is in good agreement with the experimental data of $ValLi^+•(H_2O)_2$. The observed blue shift in frequency of the free COO−H stretch at 3569 cm^{-1} with respect to the monohydrated cluster is in qualitative accord with the shift predicted by calculations. The water bands at 3656 and 3736 cm^{-1} are blue shifted in comparison with the monohydrated complex, which is well reproduced by calculations and indicates that the presence of second water molecule slightly weakens the electrostatic interaction with the lithium ion.

We thus conclude that the spectrum of $ValH^+•(H_2O)_2$ is consistent with two possible charge-solvated structures, where the lithium cation is either NO-coordinated (L2•A) or OO-coordinated (L2•B) to neutral valine. There is no experimental evidence to support a salt-bridge OO-coordinated conformation (L2•C).

(iii) $ValLi^+•(H_2O)_3$. The observed infrared spectrum of $ValLi^+•(H_2O)_3$ (Figure 11) is substantially different from that of $ValLi^+•(H_2O)_{1-2}$. The free COO−H stretch absorption disappears, and the relative intensities of the two free water O−H stretches at 3659 cm^{-1} and 3738 cm^{-1} are reversed, with the anti-symmetric stretch band more intense than the symmetric stretch. These bands are slightly blue shifted from their position in the spectrum of $ValLi^+•(H_2O)_2$, suggesting a weakened ion−dipole interaction probably originating from the presence of an additional water molecule around the metal ion. New bands arise at 3444 and 3619 cm^{-1}, and the CH stretch absorption band at 2980 cm^{-1} gains in relative intensity.

The calculated minimum energy conformation (L3•D) exhibits NO coordination of the lithium cation surrounded by two

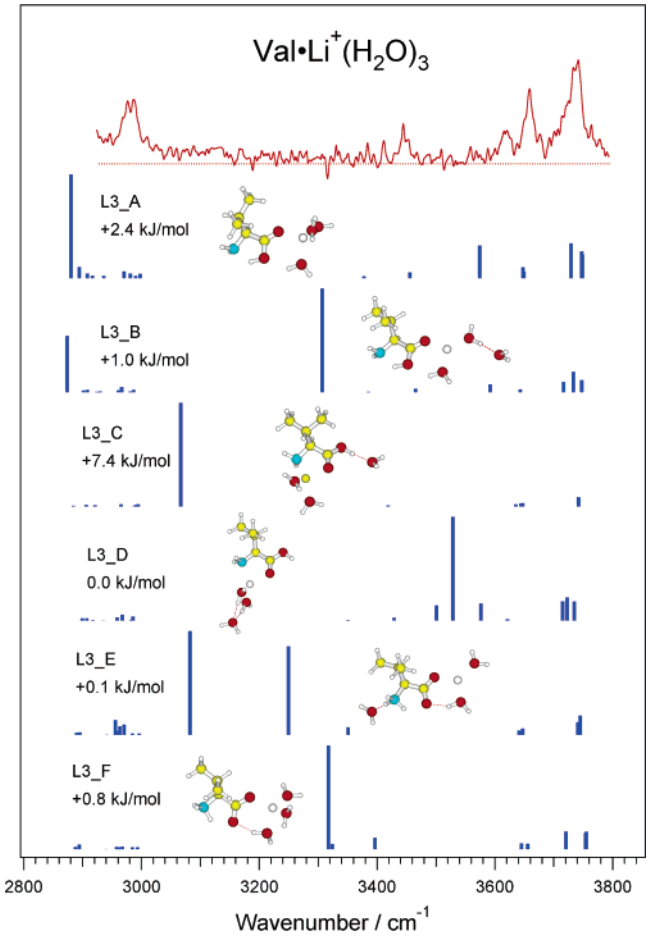

Figure 11. Comparison of measured infrared spectrum of Val·$Li^+(H_2O)_3$ with calculated spectra corresponding to the structures shown.

inner-shell water molecules bonded to an outer-shell water (AA), forming a cyclic structure. The disappearance of the free COO−H absorption from the spectrum clearly contradicts the possible occurrence of such a conformer. Moreover, the hydrogen-bonded O−H stretch bands of the two inner-shell water molecules, which are predicted by calculations to occur around 3500−3600 cm^{-1}, do not appear in the measured spectrum.

The lowest energy zwitterionic structure (L3•E) differs only by 0.1 kJ/mol from the minimum energy structure (L3•D). In such a conformation the lithium is OO-coordinated and surrounded by two water molecules, one of which donates a hydrogen to the carboxylate group, and the third water hydrates the ammonium group. The spectrum corresponding to L3•E is consistent with the observed disappearance of the COO−H stretch, but it cannot account for the appearance of bands at 3619 and 3444 cm^{-1}. Moreover, the observed spectrum shows no sign of the hydrogen-bonded ammonium bands in the 3000 cm^{-1} region that were so prominent in the spectra of the $ValH^+\cdot(H_2O)_n$ clusters. An alternative zwitterionic structure (L3•F) in which the third water fills the first solvent shell of Li^+ rather than hydrating the ammonium group of valine is energetically competitive, but there seems to be no feature in the observed spectrum that corresponds to the strong hydrogen-bonded OH water stretch predicted to appear at 3310 cm^{-1}. Thus, the experimental data are not consistent with the calculated spectra for the two salt-bridge structures, even though they are predicted to be among the most stable. We therefore need to examine higher energy conformers.

Only one low-energy structure (L3•C) exhibits NO coordination of the lithium ion. This conformer derives from L2•A, one of the two dominant conformers contributing to the spectrum of $ValLi^+\cdot(H_2O)_2$, with the third water molecule hydrogen bonded to the carboxylic acid OH. While this interaction will shift the COO−H stretch away from the 3600 cm^{-1} region, consistent with the observed spectrum, we do not observe the intense, shifted band in the region of 3100 cm^{-1} where it is predicted to occur. All other stable conformers derive from the OO-coordinated conformer L2•B identified in the doubly hydrated cluster. The most stable among these conformers (L3•B) possesses an outer-shell water molecule that would give rise to an intense band around 3300 cm^{-1}, contrary to the observed spectrum. Finally, the OO-coordinated conformer (L3•A), possessing a complete first solvent shell around Li^+ with three water molecules, seems to agree best with the experimental spectrum. The hydrogen-bonded water bridging the carboxylic acid is consistent with the absorption band at 3619 cm^{-1}, and the NH stretches calculated around 3400 cm^{-1} can account for the observed band at 3444 cm^{-1}. Furthermore, the presence of two free water molecules correlates with the high-frequency absorption bands in the measured spectrum.

(iv) $ValLi^+\cdot(H_2O)_4$. The spectrum of $ValLi^+\cdot(H_2O)_4$ (see Figure 3d) shows evidence for two main absorption bands, one above 3700 cm^{-1} characteristic of a free O−H band and the other centered at 3450 cm^{-1}, which may be due to hydrogen-bonded stretches of AD water molecules. The breadth of these bands suggests the presence of many transitions falling within the same band. The disappearance or very weak contribution of the symmetric O−H stretch implies the loss of free water O−H stretches which would result from the formation of a second solvent shell. The spectral features from 3400 to 3800 cm^{-1} are remarkably similar to those of $ValH^+\cdot(H_2O)_4$. By analogy with protonated valine clusters (Figure 8) we might assume that a cyclic structure forms with two AD waters bound to a terminating AA water, giving rise to the absorption bands between 3400 and 3560 cm^{-1}. The strong and narrower absorption band of the free OH stretches at 3738 cm^{-1} corroborates the formation of such a symmetric H-bonded structure.

V. Discussion and Conclusions

Having looked in some detail at our measured infrared spectra and compared them with calculations of spectra for different structures, we present here an overview of the solvation process for both the protonated and lithiated valine−water clusters. It is clear that at the level of B3LYP/6-31++G** the predicted lowest energy structures do not always have a spectrum that best corresponds to what we measure—it is often the case that the spectra of slightly higher energy structures agree much better. While this should not be surprising given the general uncertainties in the calculated energies, there can be systematic biases to the calculated results. In particular, the stabilization arising from hydrogen bonding to the carboxylic OH seems to be systematically overestimated with respect to putting a second water molecule on a protonated ammonium. Nevertheless, the calculations provide invaluable guidance in predicting the spectrum that would correspond to a particular structure. While

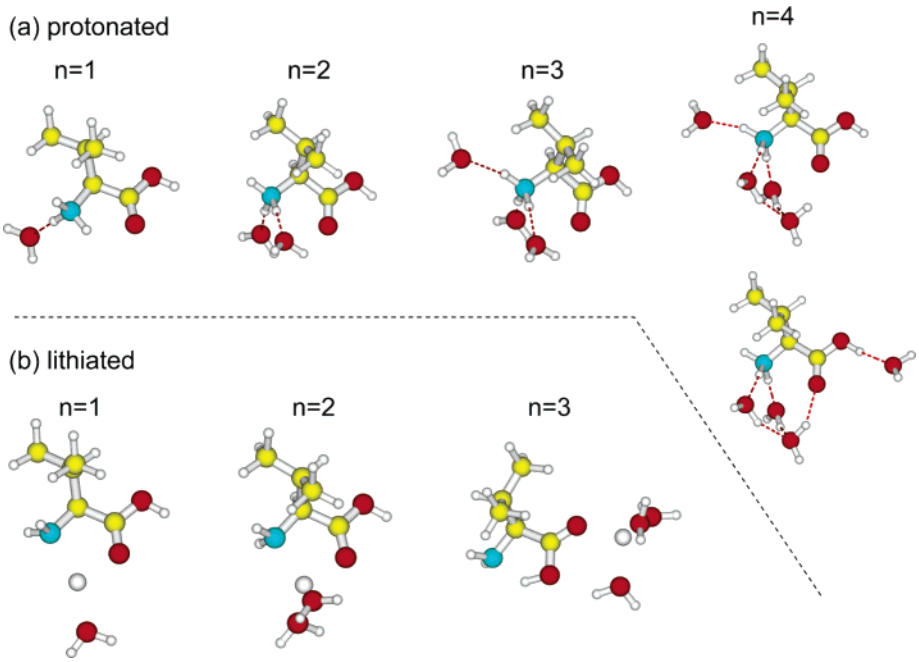

Figure 12. Overview of the solvation process in both the protonated and the lithiated valine.

the intensities of the bands do not seem to be particularly well predicted, where we have clear assignments of the observed bands the calculated band positions correspond well to what we observe. The calculations also seem to predict the disappearance of high-frequency stretch bands that are red shifted outside the frequency range of our spectra upon hydrogen bonding with water as well as more subtle blue shifts of free water OH bands upon addition of water to the same charge site. In our discussion below we use the structures that agree best with the observed spectra to interpret the stepwise solvation of protonated and lithiated valine−water clusters.

The data shown in Figures 5−11, together with the calculated structures and spectra, suggest that the solvation process is driven by the charged group in preference to hydrogen-bonding sites on the amino acid. We show this schematically in Figure 12.

For the protonated species the first three water molecules seem to preferentially bind to the protonated ammonium. In the case of the fourth water molecule, we cannot clearly distinguish between two structures. In both cases there seems to be a second solvation shell being formed in which one water molecule binds to two others that are bound to the ammonium. In the lowest energy structure the remaining water molecule is bound to carboxylic acid OH, while in a higher energy structure that water is bound to the ammonium. Our experience tells us that the calculations overestimate the stabilization due to hydrogen bonding on the carboxylic site, and our intuition tells us that solvation of the ammonium should be preferred. This being the case, the overall picture is that solvation takes place at the charge site until the first solvation shell is filled, and then water begins to form a second shell, binding to other waters rather than to sites on the amino acid backbone.

In the case of the lithiated species the situation is similar—solvation occurs preferentially at the lithium ion for the addition of the first three water molecules. While we do not have calculated spectra for Val·$Li^+(H_2O)_4$, the strong resemblance with the spectrum of the corresponding protonated species

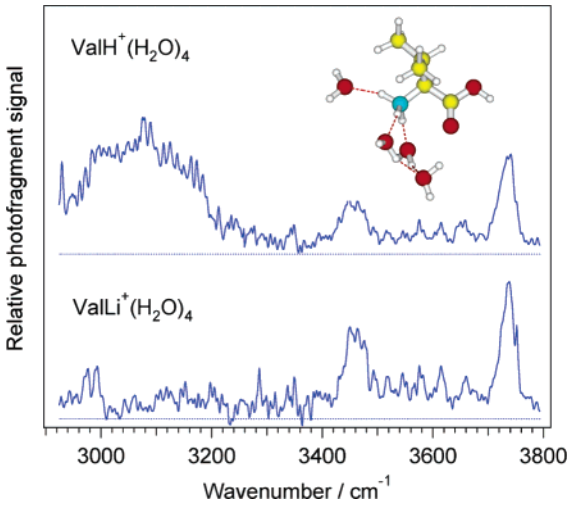

Figure 13. Comparison of the quadruply hydrated protonated and lithiated species.

suggests that a similar extended water structure is formed. This can be seen most clearly in Figure 13, where the correspondence between almost every feature in the range 3450−3750 cm^{-1}, where we expect hydrogen-bonded water bands to occur, is striking.

Given the similarity of the solvation process for protonated and lithiated valine, we might expect to see similar trends in other amino acids with uncharged side chains, as polar groups do not seem to compete with solvation of the charge or with water itself. Indeed, in spectra that we have measured for protonated tryptophan, the indole N−H stretch shows no sign of hydrogen bonding.

An interesting feature of the solvation process in the lithiated species is the apparent change in amino acid backbone conformation upon addition of the third water molecule—from the syn to the anti configuration. For Val·$Li^+(H_2O)_2$ calculations predict that the two conformers have roughly equal energy, although the spectrum agrees slightly better with the syn

configuration. For Val·$Li^+(H_2O)_3$ the spectrum clearly points to the anti configuration for the amino acid backbone, which is stabilized by the interaction of the carboxylic OH with the lone pair on the amine nitrogen.

This difference in amino acid backbone conformation between Val·$Li^+(H_2O)_2$ and Val·$Li^+(H_2O)_3$ and the associated change in lithium ion location from NO coordination to OO coordination is consistent with conclusions from the BIRD studies of Williams and co-workers.[35,37] In these studies the change in the mode of metal ion binding from NO to OO coordination was deduced from both the dissociation kinetics as well as water binding energies to these two species in comparison to model compounds known to exist in zwitterionic or nonzwitterionic forms. These results were more consistent with a zwitterion form of valine with three water molecules. A similar change in the mode of metal ion binding occurs for both sodiated glycine and valine upon addition of a second water molecule, although the forms of the amino acids in these clusters could not be identified based on the water binding energies.[35,44] In contrast, the results presented here, which probe more directly the structure of the solvated species, show no sign of zwitterion formation in lithiated valine with addition of up to four water molecules.

The discrepancy between conclusions for the Val·$Li^+(H_2O)_3$ structure drawn from the BIRD data and those from IR spectroscopy experiments could arise from a number of factors. It is increasingly difficult to draw structural conclusions from water binding energies with increasing hydration extent due to the smaller differences in water binding energies between different structures. With BIRD structural information is inferred from these small differences and from measurements of model compounds with known structure. An excellent reference structure is available for the NO-coordinated form of Val·$Li^+(H_2O)_3$, and the change in metal ion binding between the clusters with two vs three water molecules is clearly indicated from the results of both experiments. There are no suitable reference structures for the zwitterionic form of Val·$Li^+(H_2O)_3$, and a zwitterionic structure was inferred as the most likely reason for the higher water binding energy for Val·$Li^+(H_2O)_3$ vs the nonzwitterionic and zwitterionic model compounds that had different modes of water binding. Infrared spectroscopy probes the structures of these hydrates more directly and should provide more reliable information in cases where suitable reference structures are not available. It is also possible that the structure of this ion differs in the two experiments, since this may depend on how these ions are formed (condensation of water on bare ions vs solvent evaporation of more extensively hydrated droplets),[15] the internal energy of the clusters, and the time scale of the experiments. The latter two factors are clearly very different in these two experiments, and the formation mechanism could be different as well.

In summary, we have shown that infrared spectroscopy can provide valuable information on the structure of solvated biological molecules in the gas phase that complements data obtained by BIRD studies. Because of the ability of nanospray to produce a wide variety of gas-phase ions, this technique should find wide applicability. One of the main limitations of the present approach is the lack of control of the internal energy of the species under investigation, which may lead to the presence of multiple conformers. Several improvements are underway to solve this problem, including the introduction of a cooled 22-pole ion trap in place of the octopole and the implementation of multiple-laser, conformer-specific spectroscopies.

Acknowledgment. We thank the École Polytechnique Fédérale de Lausanne, the Fond National Suisse (grant no. 200020-103666/1), and the National Science Foundation (grant no. CHE-0415293) for their generous support of this work.

JA056079V